

Supporting Information to

Polarized Olefins as Enabling (Co)Catalysts for the Polymerization of γ -Butyrolactone

Patrick Walther,^a Wolfgang Frey^b and Stefan Naumann^{a*}

^aUniversity of Stuttgart, Institute of Polymer Chemistry, 70569 Germany

^bUniversity of Stuttgart, Institute of Organic Chemistry, 70569 Germany

E-Mail: stefan.naumann@ipoc.uni-stuttgart.de

Contents

Experimental.....	2
Starting materials and catalyst synthesis	2
General polymerization procedures.....	4
Characterization and analysis.....	4
Characterization of 1,3-dimesityl-2-methylene-tetrahydropyrimidine (NHO 6).....	5
Organopolymerization of γ -butyrolactone	13
Dual catalytic polymerization of γ -butyrolactone	16
References	24

Experimental

Starting materials and catalyst synthesis

γ -Butyrolactone (GBL, TCI Chemicals, > 99.0 % (GC)) was dried over CaH_2 , and subsequently distilled under static vacuum ($1 \cdot 10^{-3}$ mbar). After degassing the clear liquid with two cycles of freeze-pump-thaw, GBL was stored under protective conditions inside the glove box (LabMaster, MBraun, Germany, freezer, -36 °C). LiCl (Sigma Aldrich, powder, ≥ 99.99 % trace metals basis), MgCl_2 (Alfa Aesar, “ultra dry”, 99.9 %), YCl_3 (Alfa Aesar, “ultra dry”, 99.99 %, ampouled under argon) and ZnI_2 (Acros, “extra pure”, 99.999 %) were used as received and stored inside the glove box under exclusion of light. The solvents used in polymerization reactions were taken from a solvent purification system (MBraun, Germany), and stored under protective conditions (glove box) over molecular sieves (3 Å).

If not stated otherwise, the depicted *N*-Heterocyclic Olefins (NHOs, Figure S1) have been synthesized according to literature-known procedures, where also their characterization is documented.¹⁻⁵ An overview regarding the synthetic routes is provided below (Figure S2).

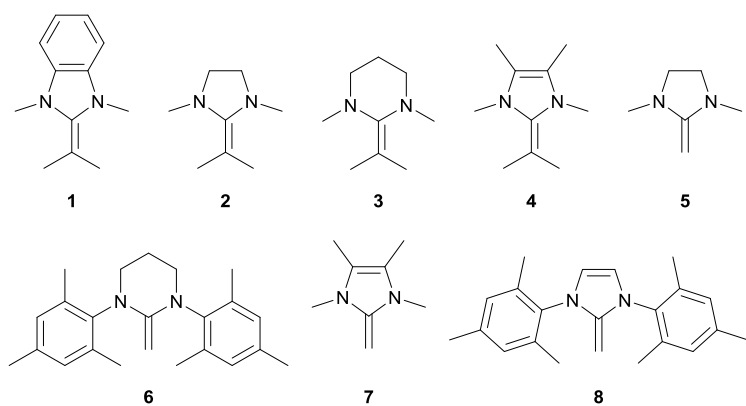


Figure S1. NHOs employed in this study.

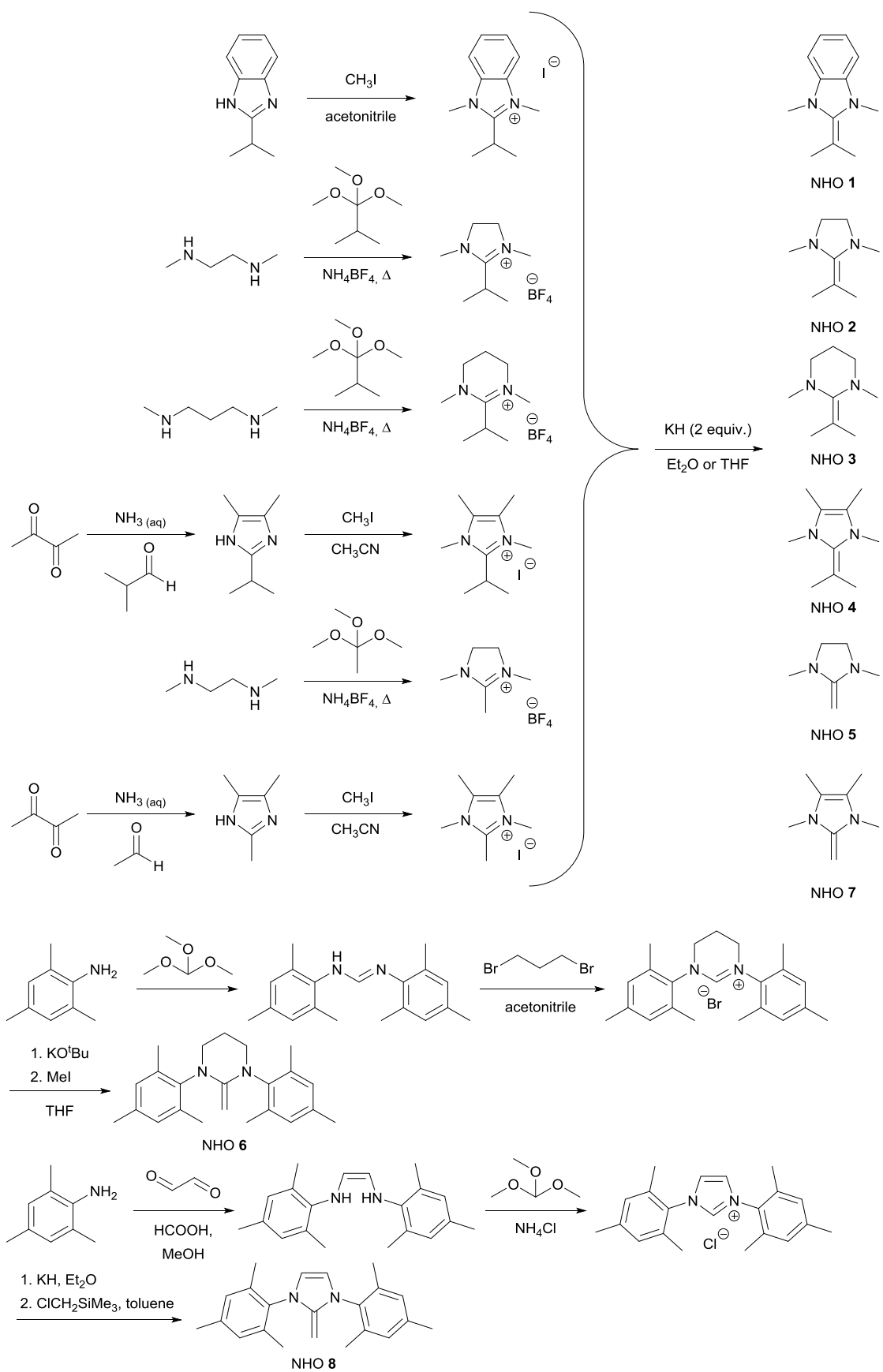


Figure S2. Synthetic routes for the NHOs employed in this study. For detailed preparation procedures, see cited references.¹⁻⁹

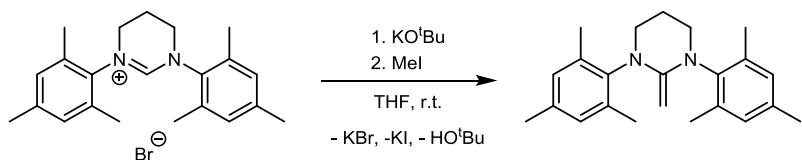
General polymerization procedures

All reactions were carried out inside the box freezer (-36°C). The polymerizations were quenched by adding acidified methylene chloride. Subsequently, the polymer was immediately precipitated in diethyl ether to afford a colourless precipitate. Prior to precipitation, conversion was determined by means of proton NMR spectroscopy, monitoring the -CH₂-O- signal of GBL (δ = 4.31 ppm) and the resulting polymer (δ = 4.07 ppm). To obtain clear reaction solutions, the Lewis acid (0.125 mmol) was dissolved in the solvent (for neat reactions, solvent = GBL) by stirring it for approx. 15 min at room temperature before adding the other component(s) (NHO (0.025 mmol), benzyl alcohol (BnOH, 0.050 mmol) and GBL (5.0 mmol)), resulting in a total molar ratio of NHO/BnOH/MX_n/GBL = 1:2:5:200.

Characterization and analysis

¹H/¹³C NMR spectra were recorded on a *Bruker* Avance III 400 spectrometer, with the chemical shifts being reported relative to reference peaks of the applied deuterated solvents (CDCl₃: δ = 7.26/77.16 ppm for proton and carbon spectra, respectively). GPC (CHCl₃, 40 °C) was used to determine the molecular weight of the synthesized poly(GBL), against a polystyrene calibration. A chromatographic assembly comprising a *PSS SDV* 5 μm 8*50mm guard column, three *PSS SDV* 100 000 Å 5 μm 8*50mm columns and an *Agilent* 1200 Series G1362A detector (RI) was used. The concentration of the prepared samples amounted to 2.5 mg/mL, and a flow-rate of 1 mL/min was applied during the analyses. MALDI-ToF MS measurements were conducted with a *Bruker* Autoflex III (337 nm, reflector mode). The samples were prepared by mixing matrix solution (2,5-dihydroxybenzoic acid, 5 mg/mL in THF), polymer solution (10 mg/ml in THF), and, where required, a solution of sodium trifluoromethanesulfonate (0.1 M in 90% acetone, 10% water) with a ratio of 2:1:2. Polystyrene standards were employed for calibration. Polymerization kinetics were observed by setting up independent reactions which were then stopped after the appropriate polymerization times.

Characterization of 1,3-dimesityl-2-methylene-tetrahydropyrimidine (NHO 6)



Following the procedure of Powers et al. for a related compound,⁴ 1,3-dimesityl-tetrahydropyrimidinium bromide (500 mg, 1.25 mmol) and KO^tBu (559 mg, 4.98 mmol, 4 eq) were combined in THF (15 mL) and stirred at room temperature for 15 min. Subsequently, methyl iodide (354 mg, 2.49 mmol, 2 eq) in THF (5 mL) was added and the resulting yellow reaction mixture was stirred over night at room temperature. After filtering the suspension, volatiles were removed *in vacuo* and the crude precipitates were extracted with *n*-pentane (2x 20 mL). Concentrating the solution upon incipient crystallisation and further storage at -36°C for 72 h resulted in colourless to greenish crystals of **6** (283 mg, 0.80 mmol, 68 %). **¹H NMR (400 MHz, C₆D₆)**: δ = 6.84 (d, *J* = 0.6 Hz, 4H, ArCH), 3.14 – 3.08 (t, *J* = 6 Hz, 4H, (RN-CH₂)₂-CH₂), 2.45 (s, 2H, H₂C=C-(NR)₂), 2.38 (s, 12H, Ar(CH₃)₄), 2.15 (s, 6H, Ar(CH₃)₂), 1.78 – 1.69 (quint, *J* = 6 Hz, 2H, RN-CH₂-CH₂-CH₂-NR). **¹³C NMR (101 MHz, C₆D₆)**: δ = 148.3 (RN₂C=NR), 141.7 (ArC), 137.1 (ArC), 136.1 (ArC), 129.9 (ArC), 54.3 (H₂C=C-(NR)₂), 46.9 ((RN-CH₂)₂-CH₂), 25.1 (RN-CH₂-CH₂-CH₂-NR), 21.1 (Ar-CH₃)₂, 18.3 (Ar-CH₃). **GC-MS (rel. intensity)**: *m/z* calc. for C₂₃H₃₀N₂ = 334.24; found: 334.2.

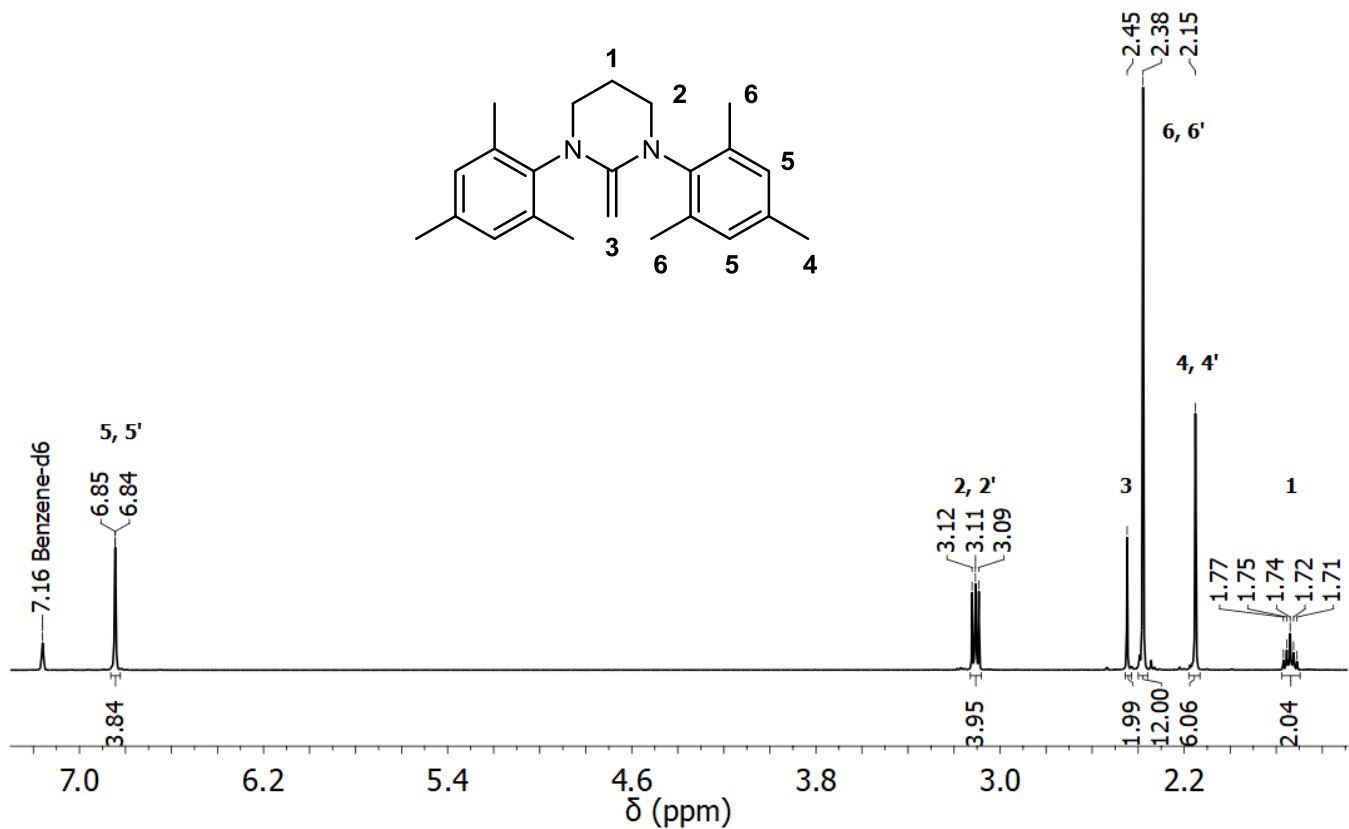


Figure S3. ¹H NMR (400 MHz, 300 K, C₆D₆) of compound **6**.

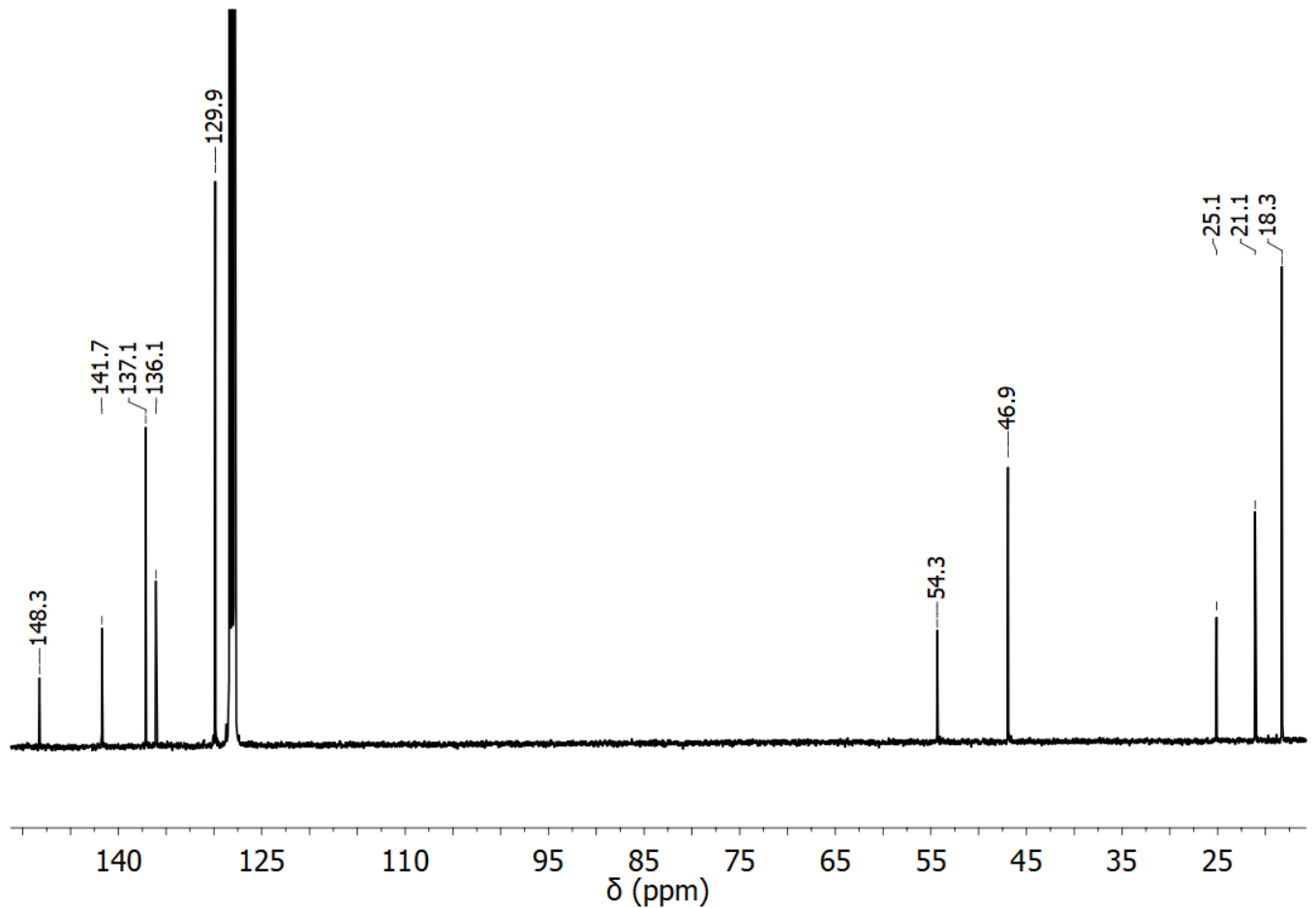


Figure S4. ^{13}C NMR (101 MHz, 300 K, C_6D_6) of compound 6.

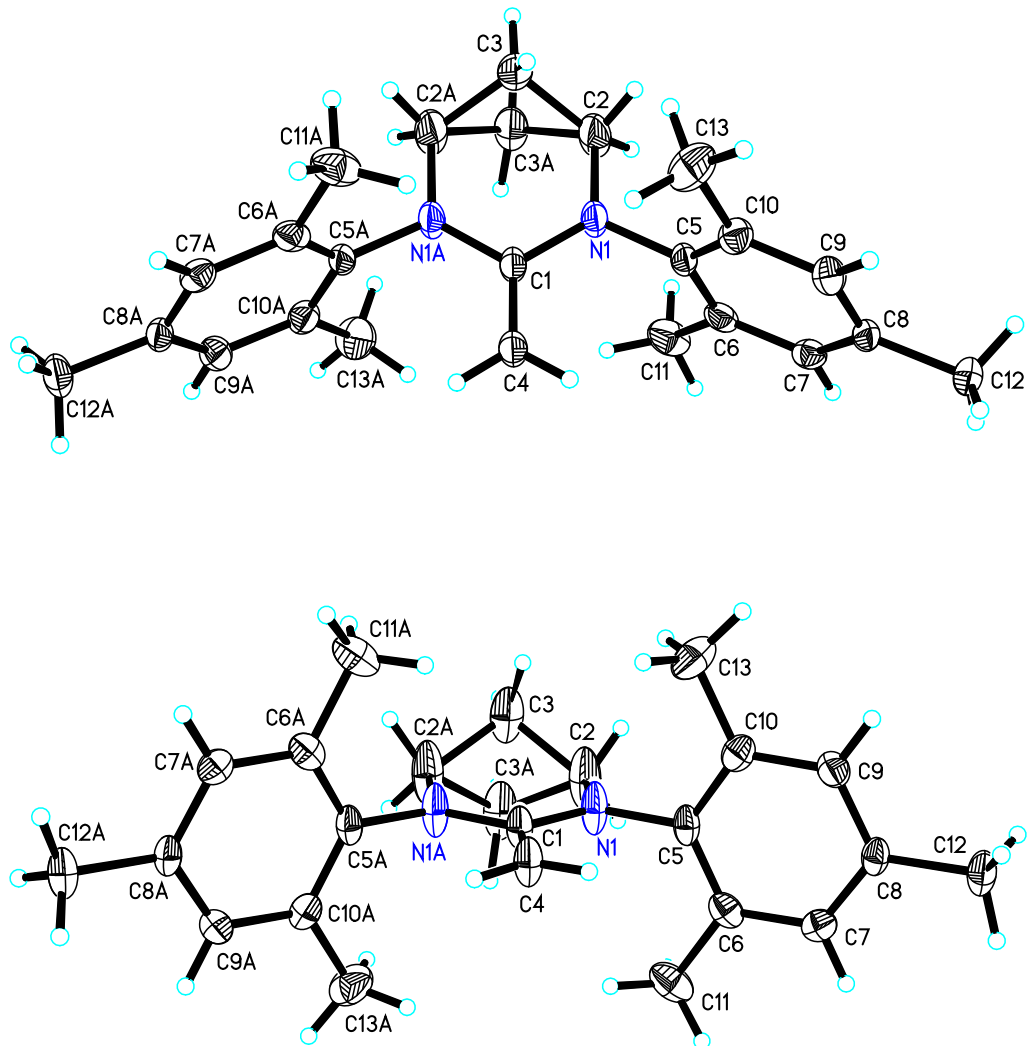


Figure S5. Single crystal x-ray structure of NHO 6.

Table S1. Crystal data and structure refinement for NHO 6.

Identification code	buch210a
Empirical Formula	C23H30N2
Formula weight	334,49
Temperature	130(2) K
Wavelength	0,71073 Å
Crystal system, space group	Orthorhombic, P b c n
	a = 15.5646(19) Å, alpha = 90 deg.
Unit cell dimensions	b = 7.8895(9) Å, beta = 90 deg.
	c = 15.9608(17) Å, gamma = 90 deg.
Volume	1959.9(4) Å ³
Z, Calculated density	4, 1.134 Mg/m ³
Absorption coefficient	0.066 mm ⁻¹
F(000)	728
Crystal size	0.57 x 0.56 x 0.09 mm
Theta range for data collection	2.55 to 28.39 deg.
Limiting indices	=-20<=h<=19 -10<=k<=9 -21<=l<=19
Reflections collected / unique	16113 / 2448 [R(int) = 0.0331]
Completeness to theta = 28.39	99.2 %
Absorption correction	Semi-empirical from equivalents
Max. and min. transmission	0.7457 and 0.7197
Refinement method	Full-matrix least-squares on F ²
Data / restraints / parameters	2448 / 3 / 132
Goodness-of-fit on F ²	1.044
Final R indices [I>2sigma(I)]	R1 = 0.0551, wR2 = 0.1529
R indices (all data)	R1 = 0.0830, wR2 = 0.1664
Largest diff. peak and hole	0.478 and -0.193 e.Å ⁻³

Table S2. Atomic coordinates (x 10⁴) and equivalent isotropic displacement parameters (Å² x 10³) for NHO 6. U(eq) is defined as one third of the trace of the orthogonalized Uij tensor.

	x	y	z	U(eq)
N(1)	406(1)	3666(2)	6881(1)	35(1)
C(1)	0	2717(3)	7500	26(1)
C(2)	383(2)	5507(2)	6843(1)	52(1)
C(3)	438(3)	6242(5)	7744(2)	45(1)
C(4)	0	1016(3)	7500	31(1)
C(5)	827(1)	2825(2)	6201(1)	23(1)
C(6)	371(1)	2446(2)	5474(1)	25(1)
C(7)	803(1)	1670(2)	4812(1)	24(1)
C(8)	1673(1)	1288(2)	4859(1)	23(1)
C(9)	2110(1)	1675(2)	5593(1)	26(1)
C(10)	1702(1)	2445(2)	6268(1)	26(1)
C(11)	-572(1)	2865(2)	5407(1)	37(1)
C(12)	2137(1)	477(2)	4130(1)	33(1)
C(13)	2189(1)	2852(3)	7061(1)	42(1)

Table S3. Bond lengths [Å] and angles [deg] for NHO 6.

N(1)-C(1)	1.3910(18)
N(1)-C(5)	1.4312(18)
N(1)-C(2)	1.454(2)
C(1)-C(4)	1.342(3)
C(1)-N(1)#1	1.3910(18)
C(2)-C(3)#1	1.550(4)
C(2)-C(3)	1.553(4)
C(2)-H(2A)	0.967(16)
C(2)-H(2B)	0.992(16)
C(3)-C(2)#1	1.550(4)
C(3)-C(3)#1	1.571(10)
C(3)-H(3A)	1.0188
C(3)-H(3B)	1.1078
C(4)-H(4A)	0.93(2)
C(5)-C(6)	1.393(2)
C(5)-C(10)	1.398(2)
C(6)-C(7)	1.394(2)
C(6)-C(11)	1.508(2)
C(7)-C(8)	1.389(2)
C(7)-H(7)	0.95
C(8)-C(9)	1.389(2)
C(8)-C(12)	1.511(2)
C(9)-C(10)	1.391(2)
C(9)-H(9)	0.95
C(10)-C(13)	1.509(2)
C(11)-H(11A)	0.98
C(11)-H(11B)	0.98
C(11)-H(11C)	0.98
C(12)-H(12A)	0.98
C(12)-H(12B)	0.98
C(12)-H(12C)	0.98
C(13)-H(13A)	0.98
C(13)-H(13B)	0.98
C(13)-H(13C)	0.98
C(1)-N(1)-C(5)	119.81(14)
C(1)-N(1)-C(2)	123.77(14)
C(5)-N(1)-C(2)	116.27(13)
C(4)-C(1)-N(1)#1	122.55(10)
C(4)-C(1)-N(1)	122.55(10)
N(1)#1-C(1)-N(1)	114.89(19)
N(1)-C(2)-C(3)#1	112.1(2)
N(1)-C(2)-C(3)	109.5(2)
C(3)#1-C(2)-C(3)	60.8(3)

N(1)-C(2)-H(2A)	110.1(15)
C(3)#1-C(2)-H(2A)	132.4(15)
C(3)-C(2)-H(2A)	85.2(14)
N(1)-C(2)-H(2B)	106.4(15)
C(3)#1-C(2)-H(2B)	89.9(14)
C(3)-C(2)-H(2B)	140.1(15)
H(2A)-C(2)-H(2B)	98.5(18)
C(2)#1-C(3)-C(2)	102.0(3)
C(2)#1-C(3)-C(3)#1	59.7(3)
C(2)-C(3)-C(3)#1	59.5(3)
C(2)#1-C(3)-H(3A)	108,7
C(2)-C(3)-H(3A)	112
C(3)#1-C(3)-H(3A)	87,1
C(2)#1-C(3)-H(3B)	112,3
C(2)-C(3)-H(3B)	101,6
C(3)#1-C(3)-H(3B)	153,3
H(3A)-C(3)-H(3B)	118,9
C(1)-C(4)-H(4A)	122.5(13)
C(6)-C(5)-C(10)	120.95(13)
C(6)-C(5)-N(1)	119.88(14)
C(10)-C(5)-N(1)	119.13(14)
C(5)-C(6)-C(7)	118.64(14)
C(5)-C(6)-C(11)	120.53(14)
C(7)-C(6)-C(11)	120.82(15)
C(8)-C(7)-C(6)	121.71(14)
C(8)-C(7)-H(7)	119,1
C(6)-C(7)-H(7)	119,1
C(7)-C(8)-C(9)	118.34(13)
C(7)-C(8)-C(12)	121.12(14)
C(9)-C(8)-C(12)	120.54(14)
C(8)-C(9)-C(10)	121.72(14)
C(8)-C(9)-H(9)	119,1
C(10)-C(9)-H(9)	119,1
C(9)-C(10)-C(5)	118.63(14)
C(9)-C(10)-C(13)	120.85(15)
C(5)-C(10)-C(13)	120.51(14)
C(6)-C(11)-H(11A)	109,5
C(6)-C(11)-H(11B)	109,5
H(11A)-C(11)-H(11B)	109,5
C(6)-C(11)-H(11C)	109,5
H(11A)-C(11)-H(11C)	109,5
H(11B)-C(11)-H(11C)	109,5
C(8)-C(12)-H(12A)	109,5
C(8)-C(12)-H(12B)	109,5
H(12A)-C(12)-H(12B)	109,5
C(8)-C(12)-H(12C)	109,5

H(12A)-C(12)-H(12C)	109,5
H(12B)-C(12)-H(12C)	109,5
C(10)-C(13)-H(13A)	109,5
C(10)-C(13)-H(13B)	109,5
H(13A)-C(13)-H(13B)	109,5
C(10)-C(13)-H(13C)	109,5
H(13A)-C(13)-H(13C)	109,5
H(13B)-C(13)-H(13C)	109,5

Table S4. Anisotropic displacement parameters ($\text{Å}^2 \times 10^3$) for NHO 6. The anisotropic displacement factor exponent takes the form: $-2 \pi^2 [h^2 a^*{}^2 U_{11} + \dots + 2 h k a^* b^* U_{12}]$

U11	U22	U33	U23	U13
N(1)	54(1)	17(1)	33(1)	0(1)
C(1)	34(1)	22(1)	23(1)	0
C(2)	83(2)	20(1)	52(1)	2(1)
C(3)	73(3)	18(2)	44(2)	-6(2)
C(4)	44(1)	20(1)	29(1)	0
C(5)	30(1)	17(1)	23(1)	2(1)
C(6)	23(1)	17(1)	34(1)	4(1)
C(7)	28(1)	20(1)	23(1)	2(1)
C(8)	29(1)	19(1)	19(1)	0(1)
C(9)	22(1)	29(1)	27(1)	1(1)
C(10)	32(1)	25(1)	20(1)	1(1)
C(11)	24(1)	29(1)	59(1)	3(1)
C(12)	40(1)	31(1)	27(1)	-6(1)
C(13)	54(1)	46(1)	26(1)	-6(1)

Table S5. Hydrogen coordinates ($\times 10^4$) and isotropic displacement parameters ($\text{Å}^2 \times 10^3$) for NHO 6.

	x	y	z	U(eq)
H(2A)	958(11)	5950(30)	6777(15)	62
H(2B)	155(14)	5810(30)	6282(12)	62
H(3A)	398	7531	7748	54
H(3B)	1031	5632	7982	54
H(4A)	294(13)	380(30)	7100(13)	45(6)
H(7)	495	1394	4317	28
H(9)	2704	1407	5635	31
H(11A)	-862	2555	5930	56
H(11B)	-826	2229	4941	56
H(11C)	-641	4082	5306	56
H(12A)	1718	133	3704	49
H(12B)	2452	-522	4327	49
H(12C)	2541	1292	3887	49
H(13A)	1974	2143	7519	63
H(13B)	2106	4050	7203	63
H(13C)	2802	2628	6975	63

Table S6. Torsion angles [deg] for NHO 6.

C(5)-N(1)-C(1)-C(4)	1.52(18)
C(2)-N(1)-C(1)-C(4)	177.05(17)
C(5)-N(1)-C(1)-N(1)#1	-178.47(18)
C(2)-N(1)-C(1)-N(1)#1	-2.95(17)
C(1)-N(1)-C(2)-C(3)#1	-27.4(3)
C(5)-N(1)-C(2)-C(3)#1	148.2(2)
C(1)-N(1)-C(2)-C(3)	38.1(3)
C(5)-N(1)-C(2)-C(3)	-146.3(2)
N(1)-C(2)-C(3)-C(2)#1	-61.5(3)
C(3)#1-C(2)-C(3)-C(2)#1	43.6(3)
N(1)-C(2)-C(3)-C(3)#1	-105.0(2)
C(1)-N(1)-C(5)-C(6)	89.75(18)
C(2)-N(1)-C(5)-C(6)	-86.1(2)
C(1)-N(1)-C(5)-C(10)	-92.30(18)
C(2)-N(1)-C(5)-C(10)	91.9(2)
C(10)-C(5)-C(6)-C(7)	0.3(2)
N(1)-C(5)-C(6)-C(7)	178.20(13)
C(10)-C(5)-C(6)-C(11)	-179.84(15)
N(1)-C(5)-C(6)-C(11)	-1.9(2)
C(5)-C(6)-C(7)-C(8)	-0.7(2)
C(11)-C(6)-C(7)-C(8)	179.38(15)
C(6)-C(7)-C(8)-C(9)	1.0(2)
C(6)-C(7)-C(8)-C(12)	-178.84(14)
C(7)-C(8)-C(9)-C(10)	-0.8(2)
C(12)-C(8)-C(9)-C(10)	179.04(15)
C(8)-C(9)-C(10)-C(5)	0.4(2)
C(8)-C(9)-C(10)-C(13)	179.88(16)
C(6)-C(5)-C(10)-C(9)	-0.1(2)
N(1)-C(5)-C(10)-C(9)	-178.02(14)
C(6)-C(5)-C(10)-C(13)	-179.62(15)
N(1)-C(5)-C(10)-C(13)	2.4(2)

Organopolymerization of γ -butyrolactone

Table S7. Variations of the organocatalyzed polymerization of γ -butyrolactone.

Entry	NHO	Time [h]	Conversion ^{a)} [%]	\overline{M}_n ^{b)}	D ^{b)}	Variation
1	2	48	15	6100	1.8	NHO:BnOH:GBL = 1:2:800, bulk
2	3	48	29	6400	2.3	NHO:BnOH:GBL = 1:2:800, bulk
3	3	24	4	-	-	THF, $[M]_0 = 10$ M
4	3	24	25	4700	1.6	toluene, $[M]_0 = 10$ M
5	3	24	3	-	-	methylene chloride, $[M]_0 = 10$ M
6	3	24	60	4100	2.2	diethyl ether, $[M]_0 = 10$ M

Conditions: -36°C, NHO:BnOH:GBL = 1:2:200 if not stated otherwise; ^{a)}determined via ^1H NMR spectroscopy; ^{b)}determined via GPC (CHCl_3).

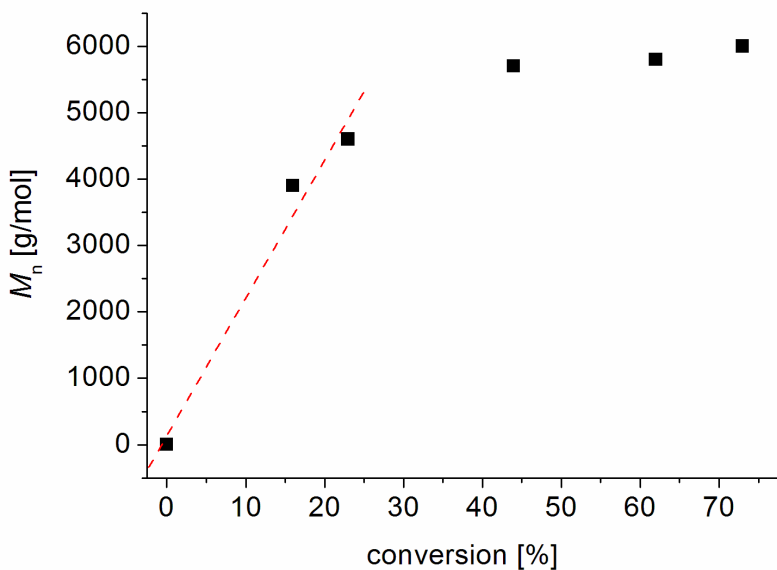


Figure S6. Correlation of M_n vs. conversion for GBL polymerization using NHO **3** with BnOH. **3**/BnOH/GBL = 1:2:200, -36°C, bulk. At higher conversion a strong deviation from linear projection occurs, probably attributable to increased backbiting and macrocycle formation (**Figure S7**).

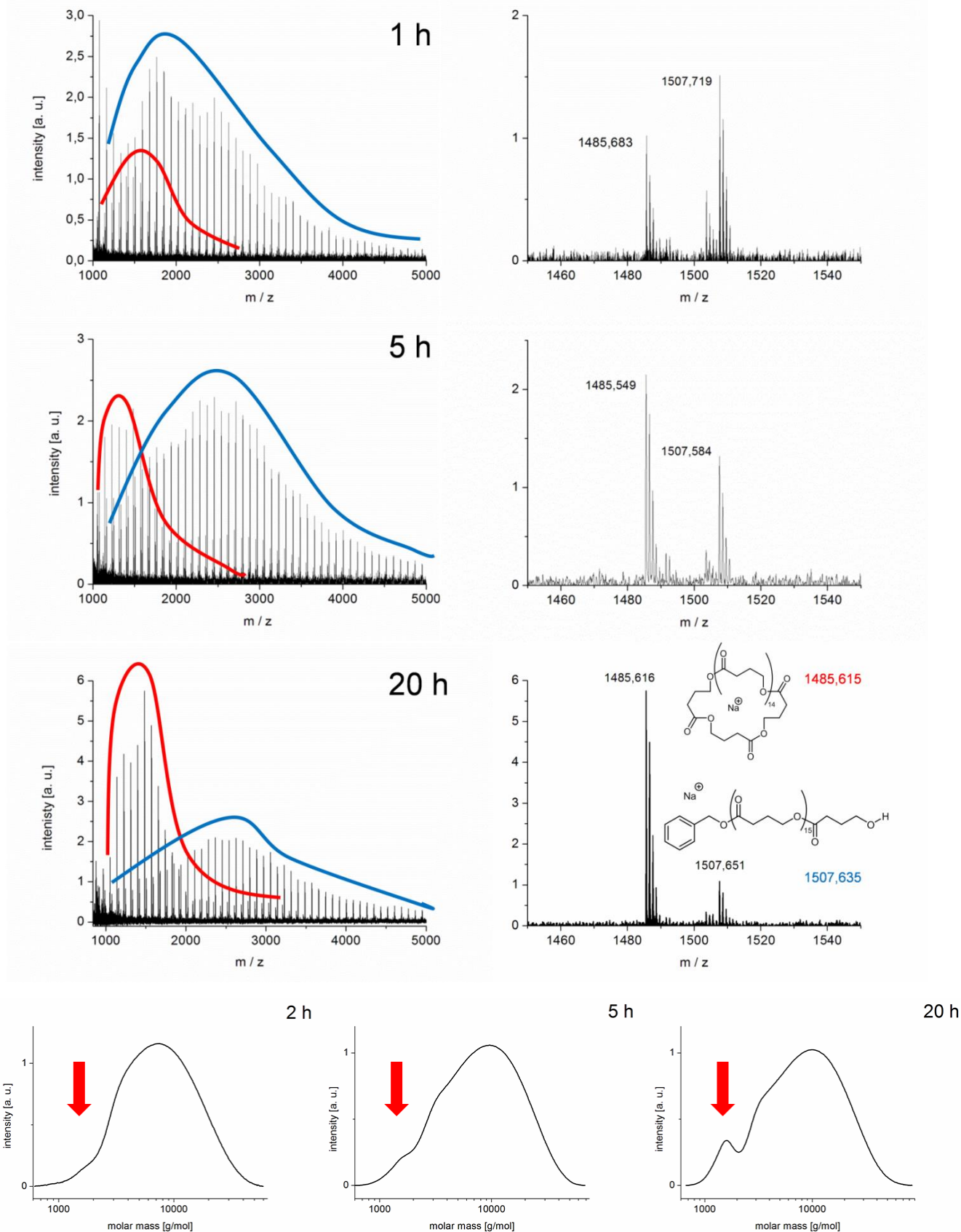


Figure S7. Organopolymerization using **3/BnOH/GBL = 1:2:200**, bulk, -36°C. Correlation of polymerization time and MALDI-ToF profiles. As the reaction proceeds, the proportion of cyclic species increases. Bottom: Corresponding chromatograms. Over time, a low-molecular weight peak is gaining intensity. In analogy to MALDI-TOF MS analysis, this mirrors the increasing proportion of macrocyclic poly(GBL) as the polymerization proceeds.

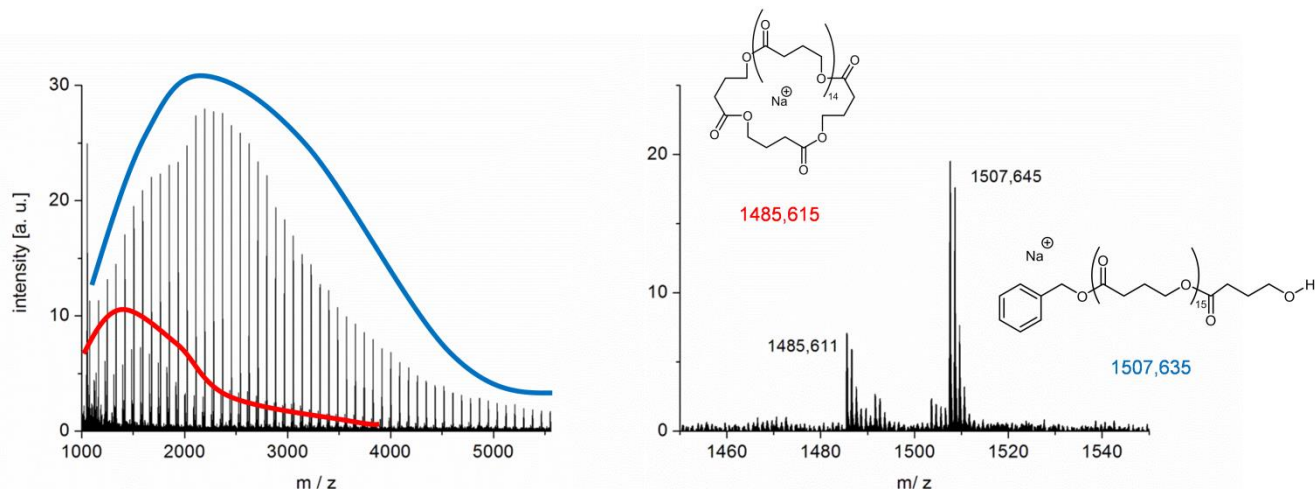


Figure S8. MALDI-ToF MS analysis of reaction **6**/BnOH/GBL = 1:2:200, bulk, -36°C, 48 h. A mixture of linear and cyclic species is received.

Table S8. Control reactions conducted without initiator (BnOH).

Entry	NHO	Time [h]	Conversion ^{a)} [%]
1	1	72	-
2	2	72	-
3	3	96	-
4	4	96	-
5	5	72	-
6	6	72	-
7	7	72	-
8	8	72	-

Conditions: -36°C, bulk, NHO/GBL = 1:200; ^{a)}determined via ¹H NMR spectroscopy.

Dual catalytic polymerization of γ -butyrolactone

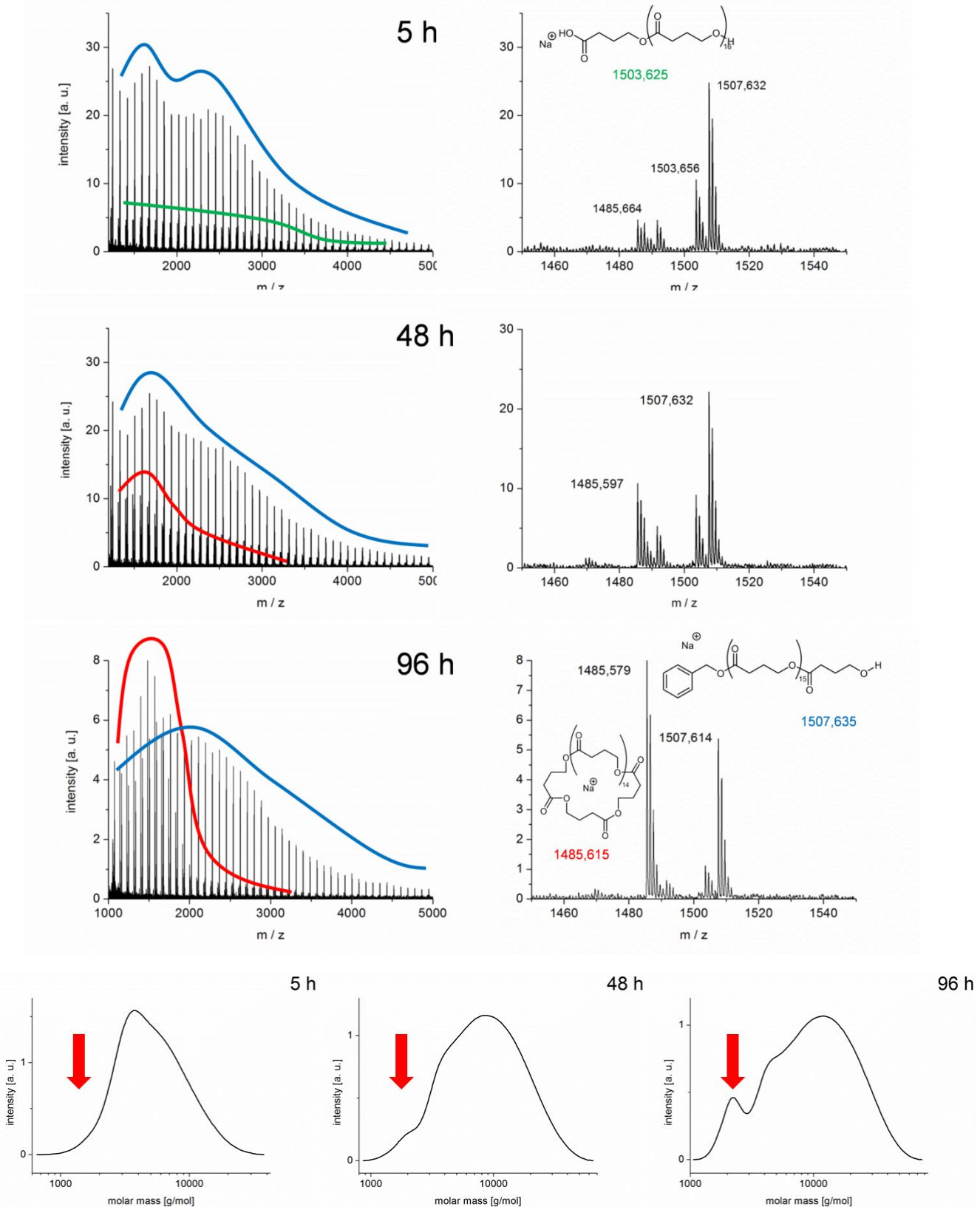


Figure S9. MALDI-ToF MS analysis of **3**/BnOH/LiCl/GBL = 1:2:5:200, bulk, -36°C. The proportion of the cyclic polymer population increases over time, yet much slower than in the analogous reaction without LiCl (compare **Figure S7**). The population marked green is OH/H terminated, most probably a result of hydrolysis in the acidic MALDI-ToF matrix. Bottom: Corresponding GPC traces, also displaying a low-molecular weight peak increasing over time.

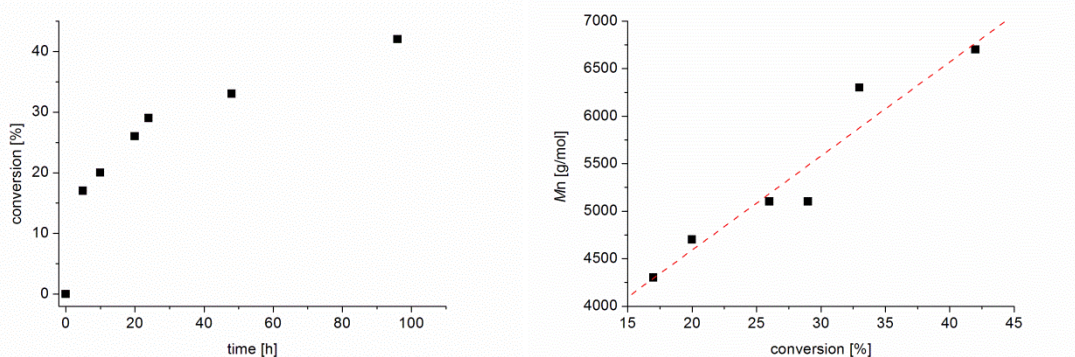


Figure S10. Correlation of conversion vs. time and M_n vs. conversion for **3**/BnOH/LiCl/GBL = 1:2:5:200, bulk, -36°C.

Table S9. Polymerization of GBL using lithium iodide (LiI) as cocatalyst. NHO/BnOH/LiI/GBL = 1:2:5:200, -36°C, bulk.

Entry	NHO	Time [h]	Conversion ^{a)} [%]	M_n ^{b)}	D ^{b)}
1	1	48	9	1400	1.76
2	2	48	27	4200	1.45
3	3	48	24	4500	1.46
4	4	48	-	-	-
5	5	48	-	-	-
6	6	48	16	3700	1.45
7	6	72	20	4500	1.33
8	7	48	15	2300	1.40
9	8	48	16	3800	1.38

^{a)}determined via ^1H NMR spectroscopy; ^{b)}determined via GPC (CHCl_3).

Table S10. Polymerization of GBL using lithium triflate (LiOTf) as cocatalyst. NHO/BnOH/LiOTf/GBL = 1:2:5:200, -36°C, bulk.

Entry	NHO	Time [h]	Conversion ^{a)} [%]	M_n ^{b)}	D ^{b)}
1	1	48	29	5200	1.42
2	2	48	27	4700	1.40
3	3	48	19	4500	1.40
4	4	48	9	3100	1.30
5	5	48	28	4300	1.47
6	6	48	19	4800	1.38
7	6	72	28	5800	1.43
8	7	48	18	4400	1.39
9	8	48	11	4400	1.34

^{a)}determined via ^1H NMR spectroscopy; ^{b)}determined via GPC (CHCl_3).

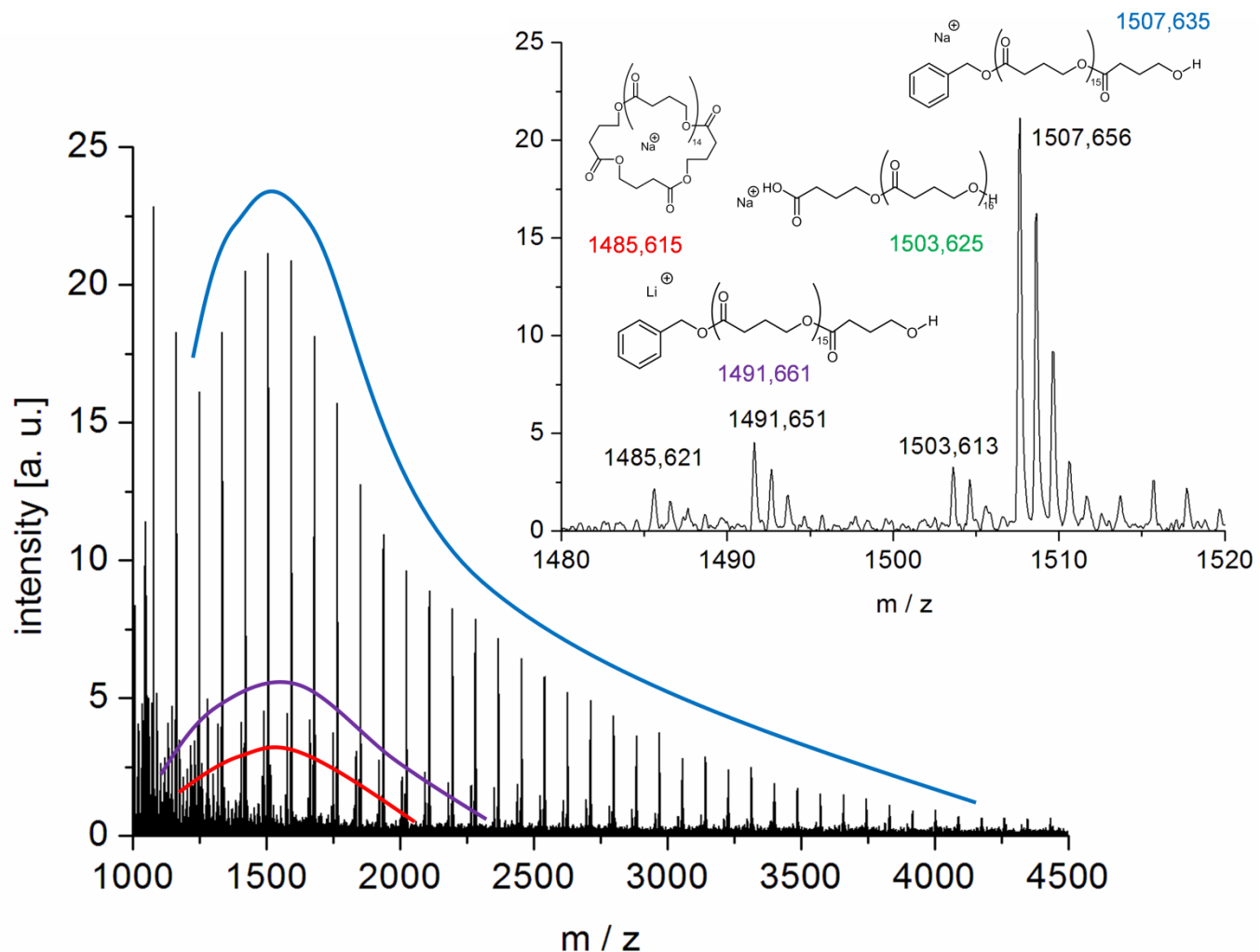


Figure S11. MALDI-ToF profile as received by the action of **6**/BnOH/LiI/GBL = 1:2:5:200, bulk, -36°C, 72 h. Even after prolonged reaction time, the linear species terminated by the initiating BnOH stays the dominating population (cationized either by sodium or by residual lithium). The OH/H-terminated fraction (green) can result from hydrolysis of either macrocyclic or linear polyester chains, most probably during matrix preparation.

Table S11. Polymerization of GBL in the presence of lithium salt but absence of BnOH, using different NHOs. NHO/LiX/GBL = 1:5:200, bulk, -36°C.

LiX	NHO	Time [h]	Conversion ^{a)} [%]	M_n ^{b)}	\overline{D} ^{b)}
LiCl	4	72	16	5800	1.6
LiCl	5	48	23	4500	3.9
LiCl	6	48	6	-	-
LiCl	6	72	13	9000	2.4
LiCl	7	72	15	3000	1.9
LiCl	8	48	17	7500	1.6
Lil	6	48	3	1600	1.7
Lil	6	72	6	2400	2.2
LiOTf	6	48	2	5300	1.4
LiOTf	6	72	4	6000	1.5

^{a)}determined via ^1H NMR spectroscopy; ^{b)}determined via GPC (CHCl_3).

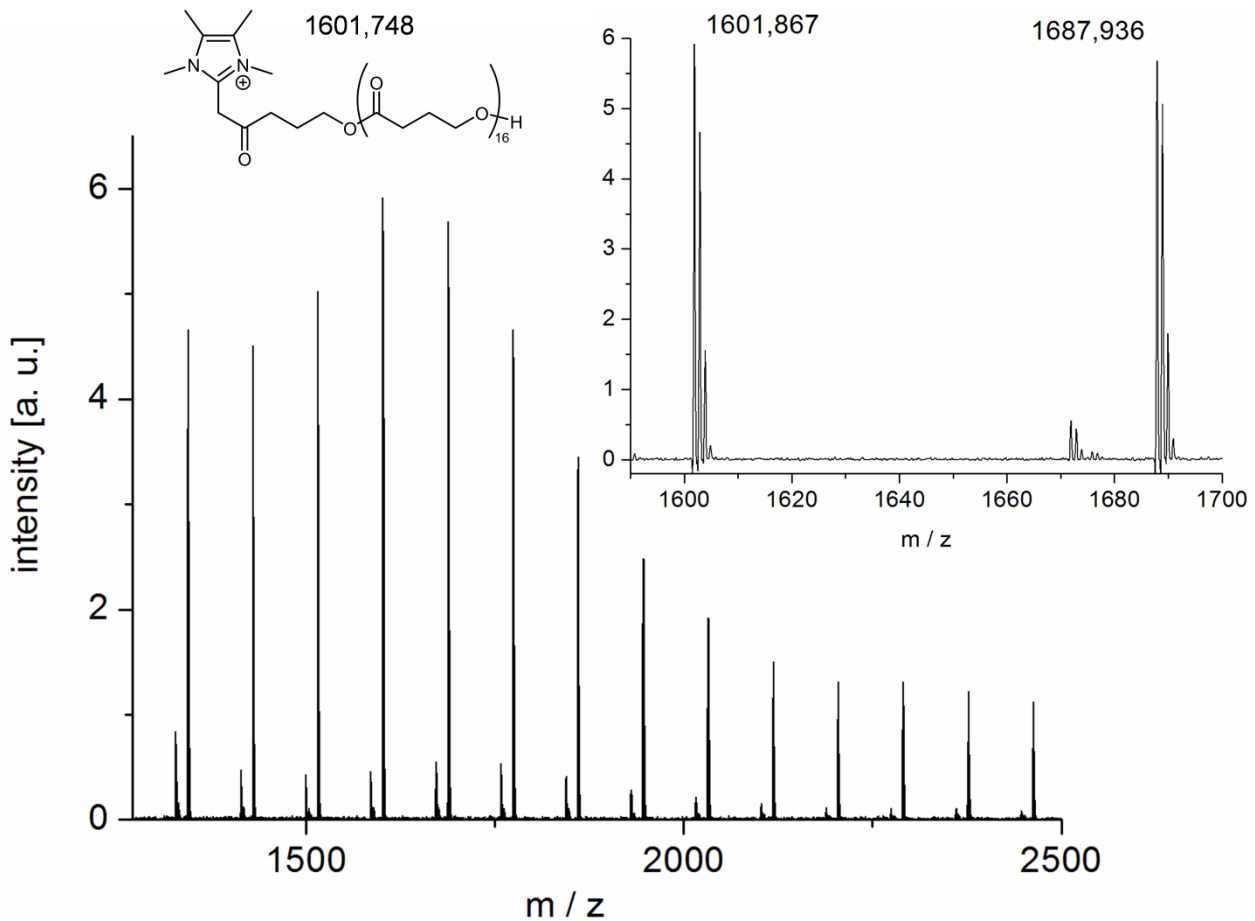


Figure S12. MALDI-ToF MS analysis of poly(GBL) prepared by the cooperative action of **7** and LiCl (**7**/LiCl/GBL = 1:5:200, bulk, -36°C). External Na⁺-cationizing agent added during matrix preparation.

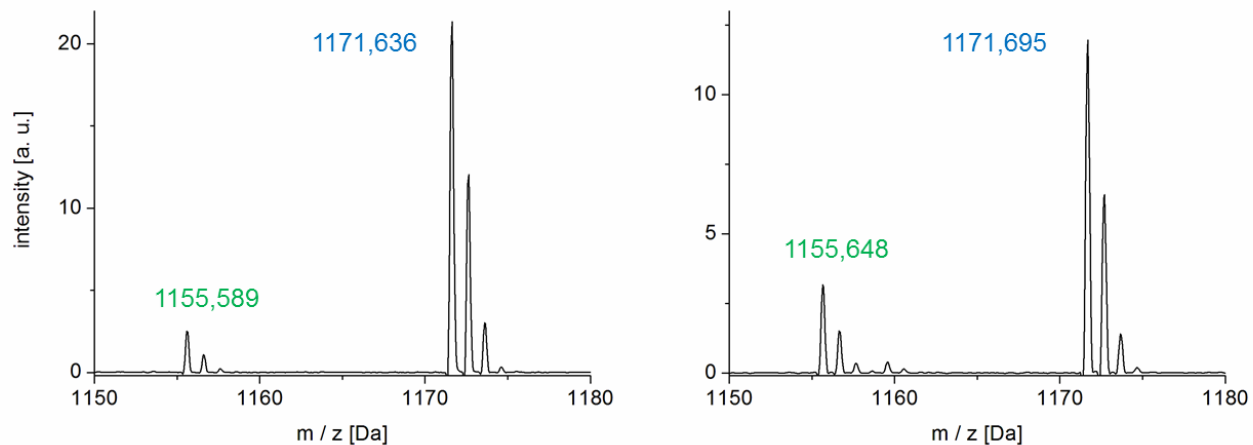
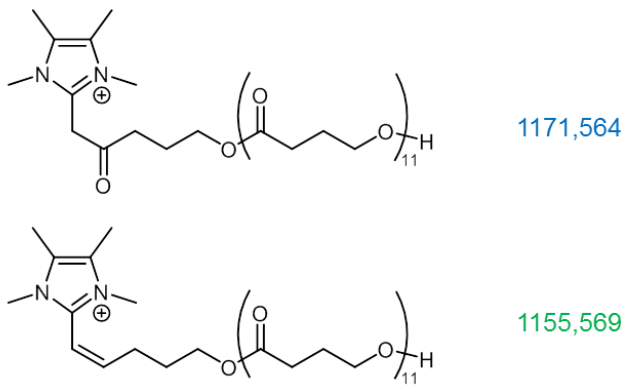


Figure S13. Detail from MALDI-TOF MS analysis regarding the poly(GBL) derived by the action of NHO 7 and LiCl (7/LiCl/GBL = 1:5:200, bulk, -36°C, compare also **Figure 2** and **Figure S12**), without (left) and with (right) Na⁺-cationizing agent added. From the data it can be concluded that also the minor population is NHO-cationized (not by Li⁺ or Na⁺). Deoxygenation, likely acid-catalyzed during matrix preparation, is proposed to account for this behaviour, generating an enlarged conjugated system.

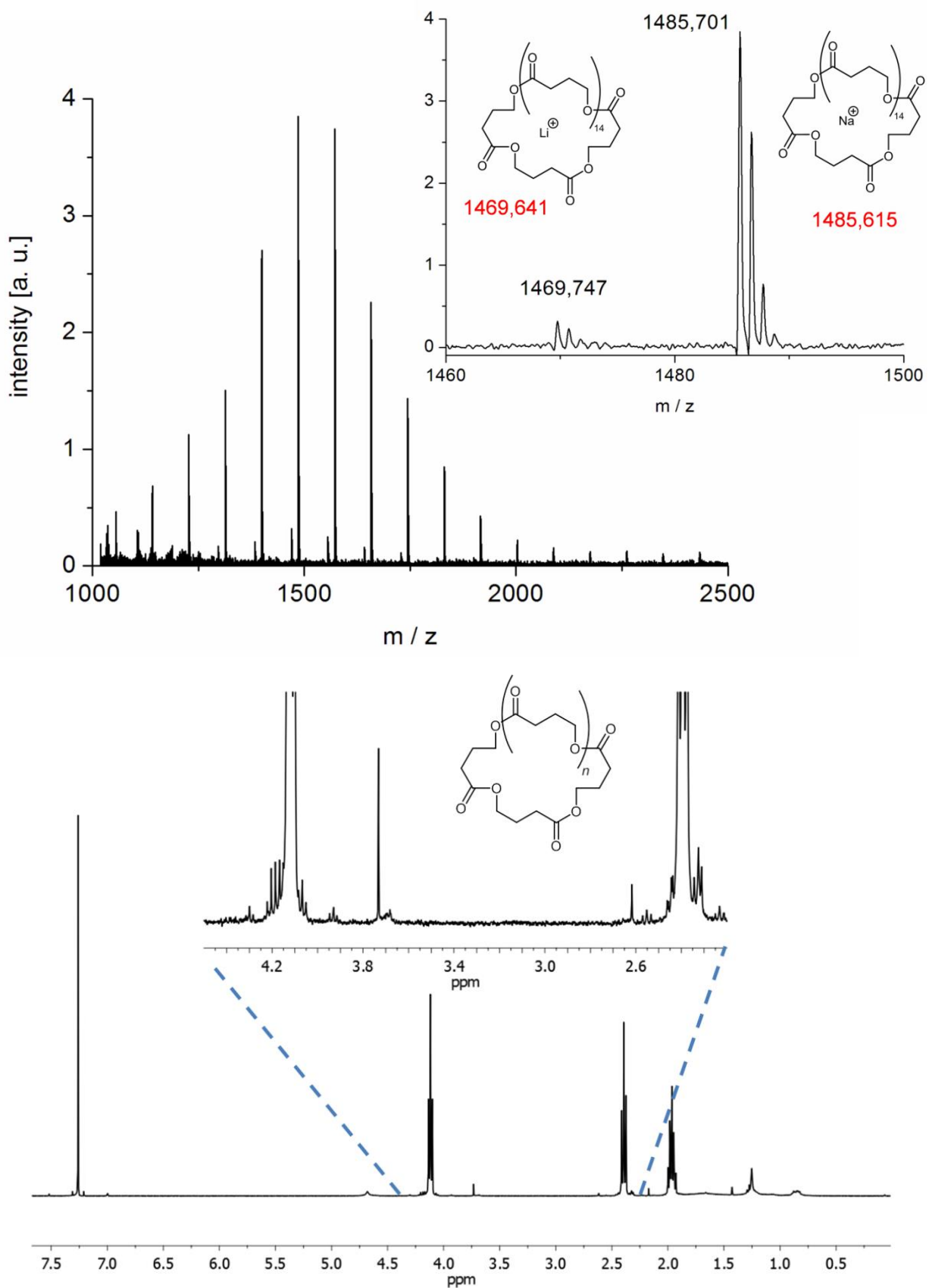


Figure S14. Top: MALDI-ToF MS analysis of poly(GBL) prepared by the cooperative action of **6** and LiCl (**6**/LiCl/BnOH = 1:5:200, bulk, -36°C, 48 h). External Na⁺-cationizing agent added during matrix preparation. Only oligocyclic species observed. Bottom: Corresponding ^1H NMR analysis (CDCl_3 , 400 MHz, 300K). Compare **Figure S15**.

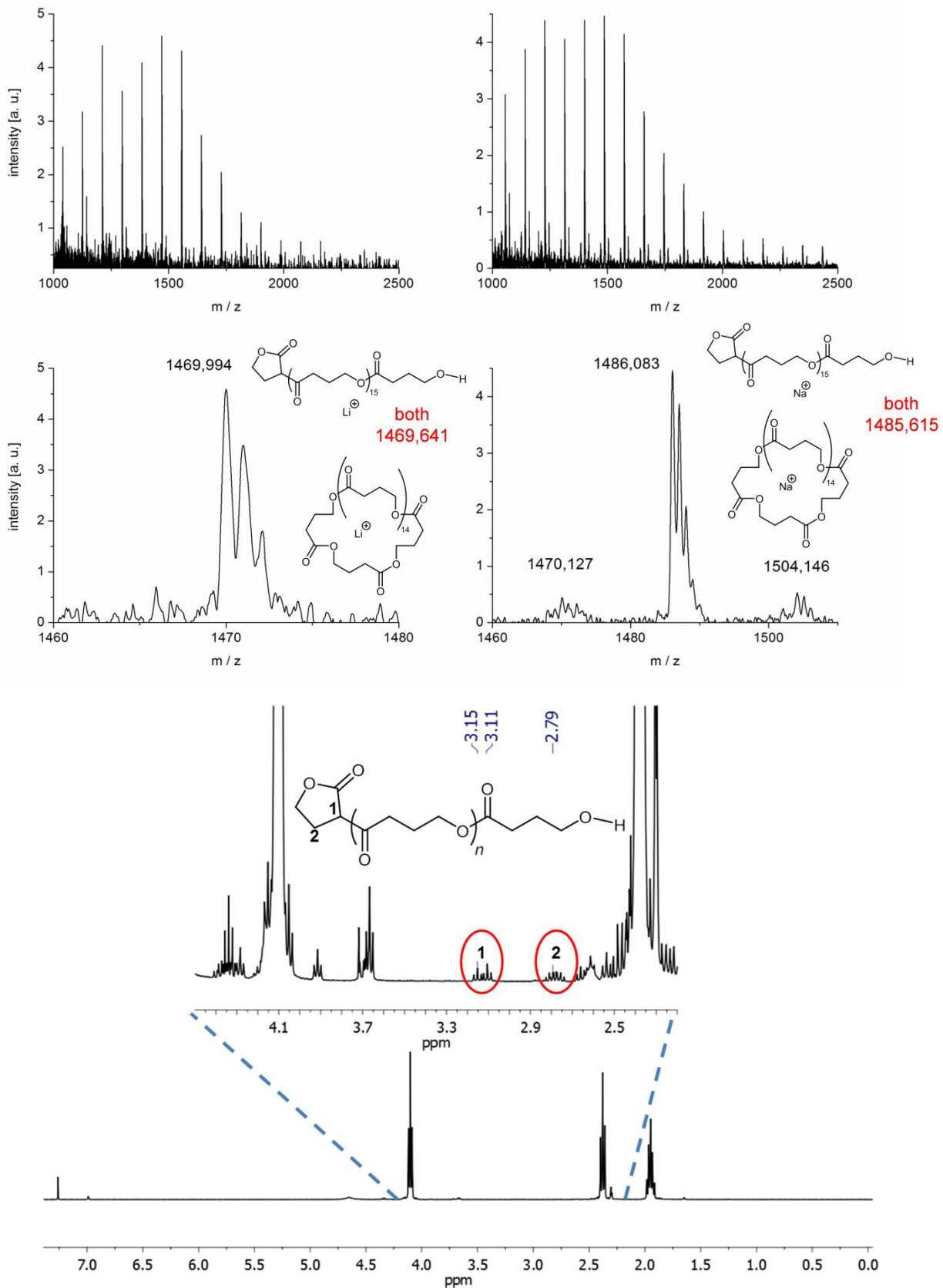


Figure S15. Top: MALDI-ToF MS analysis of polymer prepared by $\textbf{6}/\text{LiCl}/\text{GBL} = 1:5:200$, bulk, -36°C , 72 h. Measurements were conducted with (left) and without (right) specifically added Na^+ -cationizing reagent for matrix preparation. The right profile also contains a small fraction of Li^+ -cationized cyclic species and OH/H-terminated polymer (resulting from hydrolytic cleavage of ester moieties). ^1H NMR analysis (CDCl_3 , 400 MHz, 300K) and the distorted MALDI profile indicate that this is a mixture of oligocyclic and linear, enolate-derived poly(GBL). Compare **Figure S14**.

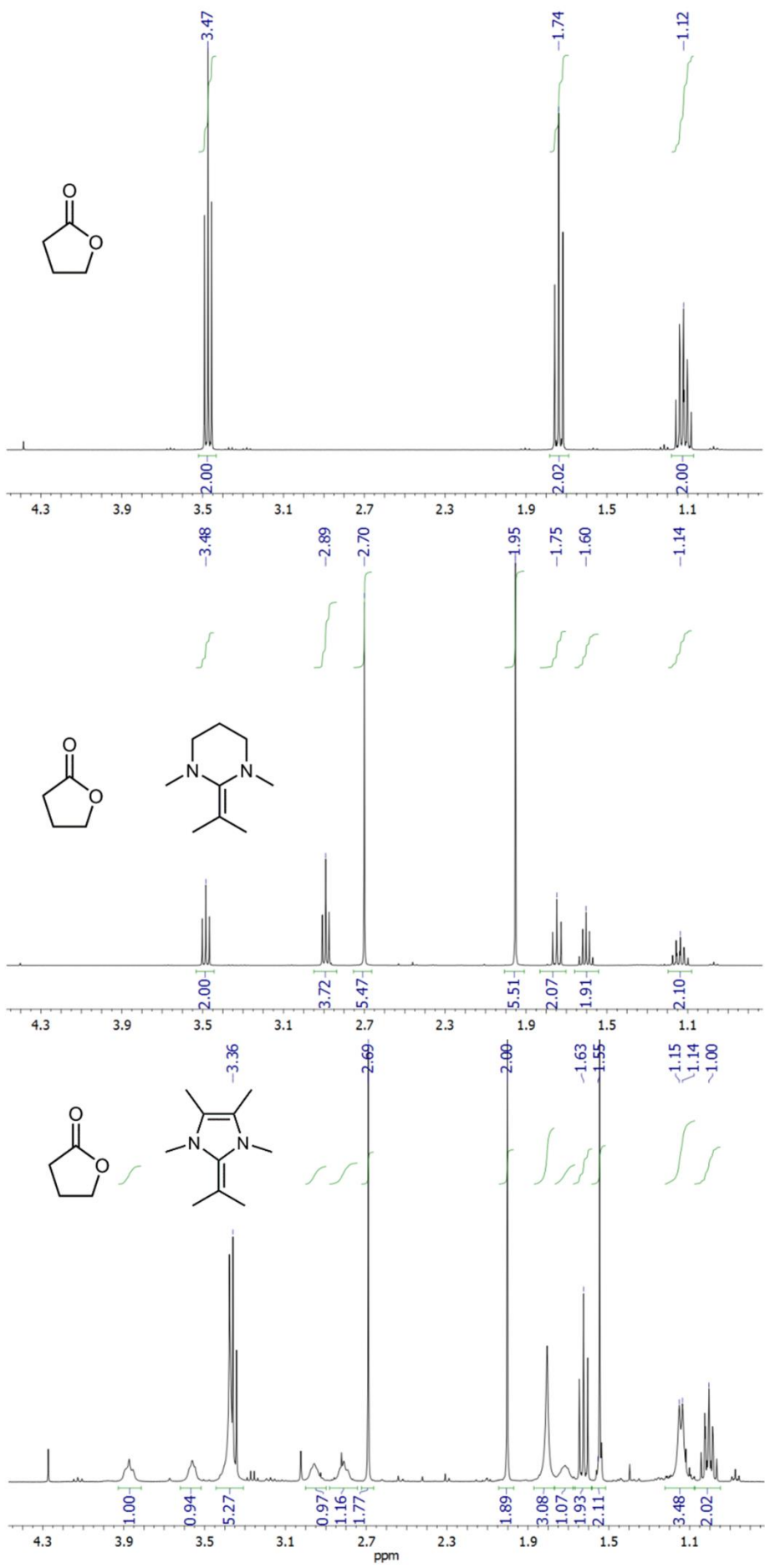


Figure S16. ^1H NMR experiments (C_6D_6 , 300 K, 400 MHz) using GBL alone (top) or in a 1:1 ratio with either NHO **3** (middle) or NHO **4** (bottom). While application of the saturated, six-membered **3** does not entail any observable changes, employment of **4** leads to a reaction. Isolation of the latter failed, but the broad doublet at $\delta = 1.14$ ppm suggests that protonation of the NHO has taken place, in turn indicating enolate formation.

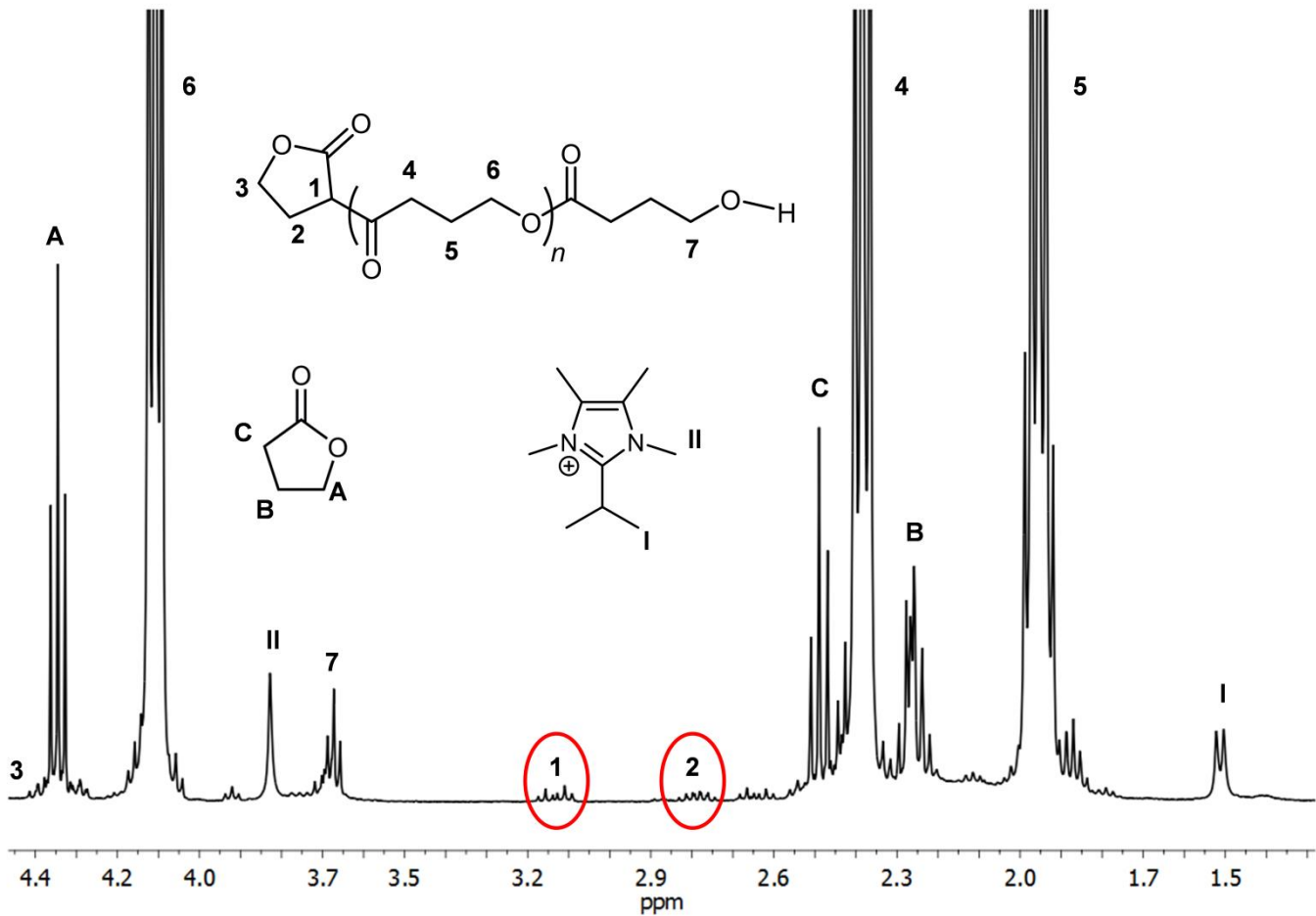


Figure S17. ^1H NMR (CDCl_3 , 300 K, 400 MHz) taken from a polymerization using **4**/LiCl/GBL = 1:5:200, bulk, -36°C. Residual amounts of non-converted GBL and protonated NHO can be observed. The signals marked **1** and **2** can be attributed to enolate-derived end groups.

References

1. U. Gruseck and M. Heuschmann, *Chem. Ber.*, 1987, **120**, 2053-2064.
2. S. Kronig, P. G. Jones and M. Tamm, *Eur. J. Inorg. Chem.*, 2013, **2013**, 2301-2314.
3. S. Naumann and D. Wang, *Macromolecules*, 2016, **49**, 8869-8878.
4. K. Powers, C. Hering-Junghans, R. McDonald, M. J. Ferguson and E. Rivard, *Polyhedron*, 2016, **108**, 8-14.
5. H. Quast, M. Ach, M. K. Kindermann, P. Rademacher and M. Schindler, *Chem. Ber.*, 1993, **126**, 503-516.
6. M. Hans, J. Lorkowski, A. Demonceau and L. Delaude, *Beilstein J. Org. Chem.*, 2015, **11**, 2318-2325.
7. C. E. Knappke, J. M. Neudorfl and A. J. von Wangelin, *Org. Biomol. Chem.*, 2010, **8**, 1695-1705.
8. K. Hirano, S. Urban, C. Wang and F. Glorius, *Org. Lett.*, 2008, **11**, 1019-1022.
9. M. Iglesias, D. J. Beetstra, J. C. Knight, L.-L. Ooi, A. Stasch, S. Coles, L. Male, M. B. Hursthouse, K. J. Cavell, A. Dervisi and I. A. Fallis, *Organometallics*, 2008, **27**, 3279-3289.